Intermittent Dissipation and Heating in 3D Kinetic Plasma Turbulence

M. Wan,[1] W. H. Matthaeus,[1] V. Roytershteyn,[2] H. Karimabadi,[3] T. Parashar,[1] P. Wu,[1] and M. Shay[1]
[1]*Bartol Research Institute and Department of Physics and Astronomy, University of Delaware, Newark, Delaware 19716, USA*
[2]*Space Science Institute, Boulder, Colorado 80301, USA*
[3]*SciberQuest, Del Mar, California 92014, USA*
(Received 2 March 2015; published 30 April 2015)

High resolution, fully kinetic, three dimensional (3D) simulation of collisionless plasma turbulence shows the development of turbulence characterized by sheetlike current density structures spanning a range of scales. The nonlinear evolution is initialized with a long wavelength isotropic spectrum of fluctuations having polarizations transverse to an imposed mean magnetic field. We present evidence that these current sheet structures are sites for heating and dissipation, and that stronger currents signify higher dissipation rates. The analyses focus on quantities such as $\mathbf{J} \cdot \mathbf{E}$, electron, and proton temperatures, and conditional averages of these quantities based on local electric current density. Evidently, kinetic scale plasma, like magnetohydrodynamics, becomes intermittent due to current sheet formation, leading to the expectation that heating and dissipation in astrophysical and space plasmas may be highly nonuniform. Comparison with previous results from 2D kinetic simulations, as well as high frequency solar wind observational data, are discussed.

DOI: 10.1103/PhysRevLett.114.175002 PACS numbers: 52.35.Ra, 94.05.-a, 96.50.Tf

The nature of collisionless dissipation in low density plasmas such as the solar wind and the solar corona has been hotly debated recently, often invoking mechanisms based on various wave modes, such as kinetic Alfvén waves, and whistlers, as well as mechanisms such as linear Vlasov instabilities, cyclotron resonance, and Landau damping [1–5]. Underlying these ideas is a premise that the plasma remains near an equilibrium and therefore that the associated dissipation is described by instabilities and noninteracting waves [2,6–8]. However, solar wind, coronal, and magnetospheric observations suggest that an appropriate description may be in terms of a turbulence cascade [1,5,9,10], which may be hydrodynamiclike "strong" turbulence, or "wave" turbulence in which some properties of the linear description persist. Indeed, magnetohydrodynamic (MHD) simulations reveal that a broadband cascade to smaller scales invariably occurs, initiated by instability [11], or by direct couplings [12]. If a sufficient spectral range is available, the dynamics can approach a self-similar "inertial range" that is terminated by collisional (viscous, resistive) dissipation at small scales. However, for a collisionless plasma, the dissipation function is unknown, and this, along with other complexities of plasma dynamics, has led to questions regarding the degree to which turbulence theory remains applicable in collisonless plasmas. Progress has been made in revealing the physical processes that terminate the inertial range, and convert cascading energy into heat—issues of fundamental importance in heating of the solar corona and forming the solar wind [9]. However, most of this progress has depended upon the use of reduced dimensionality models, reduced physics models, or very small kinetic scale systems [4,5,13–17]. It is clear that convincing answers to these crucial questions will require complete models, i.e., three space dimensions, three velocity space dimensions, and a full suite of kinetic proton and electron physics. Here we report baseline studies of plasma turbulence properties, for the first time that we are aware, using such a complete 3D kinetic model.

An important feature of plasma turbulence found in some reduced kinetic simulations [5,18–20] is that a kinetic cascade produces a hierarchy of electric current structures. Plasma dissipation is found to have a strong quantitative association with these structures. Such reduced dimensionality, or reduced physics results are instructive, but there is a high priority to extend these results into the much more computationally demanding realm of 3D kinetic simulation, which represents a grand challenge effort (e.g., [21]), and also a necessary step to achieve greater realism.

Here we report results from 3D particle-in-cell (PIC) simulations on the study of intermittency, dissipation, and heating in plasma turbulence. Consistent with earlier reduced physics results, this demonstrates that kinetic plasma dissipation in three dimensions is intermittent with dissipation largely occurring in a hierarchy of coherent structures. This lends credence to the idea that heating and dissipation in turbulent space plasmas might also be highly inhomogeneous and patchy as suggested from observations [22–24].

The present simulations employed the simulation code VPIC [25], which solves the relativistic Vlasov-Maxwell system of equations using the PIC algorithm. The initial conditions correspond to uniform plasma with density n_0, Maxwellian-distributed ions and electrons of equal temperature T_0, and uniform magnetic field $\boldsymbol{B} = B_0 \boldsymbol{e}_z$, plasma $\beta = 16\pi n_0 T_0 / B_0^2 = 0.5$. The simulation domain is a cube of size $L \approx 41.9 d_i$ with resolution of 2048^3 cells, where d_i is the ion inertial length. The ion-to-electron mass ratio is $m_i/m_e = 50$. The average number of particles/cell/species is 100, for a total of 1.7 trillion particles. Turbulence is seeded by imposing at $t = 0$ a large-scale isotropic spectrum of magnetic fluctuations having polarizations transverse to the imposed mean magnetic field, i.e., Alfvén mode fluctuations. The perturbations are equipartitioned (per mode) in a cubic k-space region including the nondimensional wave numbers $(0, \pm 1, \pm 2)$ in each Cartesian direction. The root-mean-square magnetic fluctuation amplitude is $\delta b \approx 0.316 B_0$. Further analysis and details of this simulation will appear in a companion paper [26].

The analysis we present here pertains exclusively to the dynamical state of the above described plasma after it has evolved from the initial condition for approximately 165 ion cyclotron times, which is estimated in the usual way as $\approx$1.5 characteristic nonlinear times (in units of the initial $\tau_{\mathrm{nl}} = L/Z$, where L is the energy-containing length scale and Z is the turbulence amplitude obtained from both Elsässer fields). This is after the time of maximum mean square electric current density, which in MHD would be after the time of the maximum dissipation rate, when similarity decay might be observed [27]. Note that all analyses here are done with low pass filtered data to remove counting statistics noise [19].

The first point we wish to make is that the electric current density at this time is highly structured in space, and that moreover this structure is such that one would properly call this intermittency. To this end, in Fig. 1 we show a contour of the magnitude of current density J from a transverse plane of the simulation domain. We can observe that a hierarchy of current density structures is formed, which were not present in the initial data (not shown). These structures are mainly sheetlike, with some "cores," and range from ion to electron scales. These structures are signs of coherency [26] and also of intermittency, which can be examined by calculating the probability density function (PDF) of magnetic increments for various values of the increment lag. In Fig. 1, we also show the PDF of the magnetic increments $\delta b(r) = b_y(x+r) - b_y(x)$ for different lag, or separation length r. We can observe that as r decreases from several d_i to d_e, the PDF becomes fatter with more prominent extended tails. This type of scale dependent departure from Gaussianity is generally considered to be a signature of spatial intermittency, here associated with the magnetic field.

Figure 2 shows the energy spectral density $S(k_\perp, k_\parallel)$ of the magnetic field in the $k_\perp, k_\parallel$ plane, where S is defined such that the energy density $\delta b^2 = \int S(k_\perp, k_\parallel) dk_\perp dk_\parallel$. In this figure, we plot the isocontours of S, and we can see that

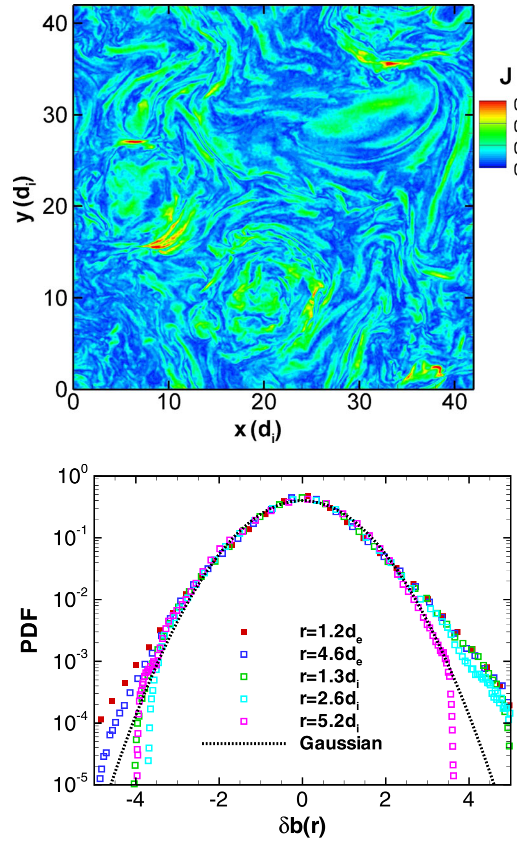

FIG. 1 (color online). (Top) Contour of the magnitude of current density J from a transverse plane of the simulation box; (Bottom) PDF of the magnetic increments $\delta b(r) = b_y(x+r) - b_y(x)$ for different separation length r.

the energy spectrum fits our expectation for anisotropic plasma turbulence: most of the energy lies close to the $k_\perp$ axis, indicating that parallel spectral transfer is suppressed, as expected in theory [28,29] and familiar in observational

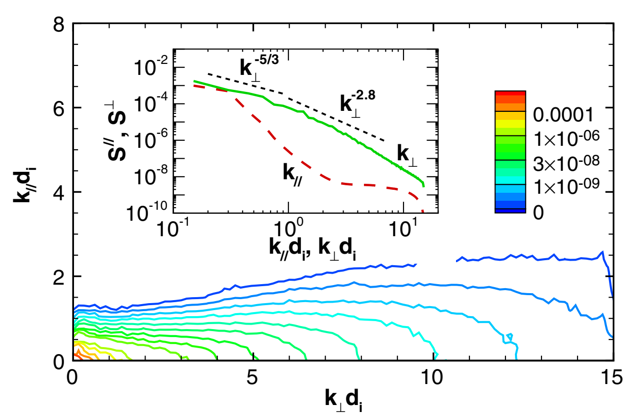

FIG. 2 (color online). Energy spectrum $S(k_\perp, k_\parallel)$ of magnetic field in the $k_\perp, k_\parallel$ plane. Inset: Parallel and perpendicular one-dimensional reduced spectra $S^\parallel$ and $S^\perp$ defined in the text. It is clear that perpendicular spectral transfer is stronger than parallel transfer.

analysis [30–32]. One may also form *reduced* spectral densities as $S^{\parallel}(k_{\parallel}) = \int dk_{\perp} S(k_{\perp}, k_{\parallel})$ and $S^{\perp}(k_{\perp}) = \int dk_{\parallel} S(k_{\perp}, k_{\parallel})$, which provides another view of the spectral anisotropy. These two spectra are shown as an inset to Fig. 2. Again, it is clear that the extension of the excitations in perpendicular wave numbers is much greater than it is in parallel wave numbers.

While spectral densities provide useful information about the turbulence cascade across scales, these second order statistics provide no spatial information about coherent structures that may influence the termination of the cascade, dissipation processes, and possible intermittency. To investigate these issues requires the detection of structures and characterizing them using statistical methods, for example, as has been done previously in 2.5D kinetic simulations [19,20], and in some 3D simulations of reconnection [33]. Lacking a simple expression for the dissipation function in a kinetic plasma, we resort to examination of quantities related to the work done by the electromagnetic field on the plasma particles. To this end we focus here on statistics related to the electric current density.

Figure 3 shows the magnitude of current density J in a close up of a small region in a transverse plane from the 3D simulation. Evidently, the regions of strong current density form a hierarchy of coherent structures extending across a wide range of scales. In the same figure, we show the contour of proton temperature T_i for the same spatial region, and the temperature is also seen to be structured, with spatial patches of both high and low values. Moreover, while the images are rather different in their details, there is a suggestion that regions of enhanced (suppressed) temperatures tend to be found in or near regions of enhanced (suppressed) current density.

We recall that the connection between dissipation and current density is precise in plasmas in which the resistive electric field is the dominant nonideal contribution to the generalized Ohm's law. In the low collisionality case, one cannot draw this conclusion. Nevertheless, it is likely that regions of high current density may be connected with

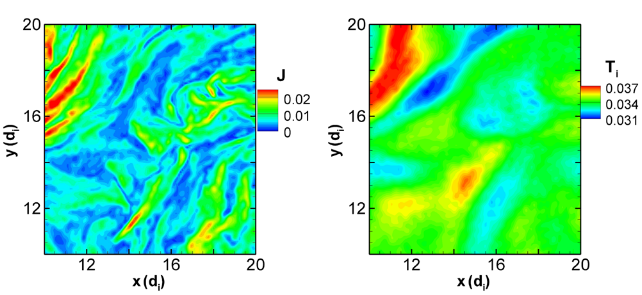

FIG. 3 (color online). (Left) Magnitude of current density J in a close-up region of a transverse plane from the simulation box showing hierarchy of coherent structures; (right) Contour of proton temperature T_i for the region shown in left.

enhanced dissipation. For example, large current density may trigger anomalous resistivity [34,35]. Indeed, recent simulations of collisionless plasma have suggested that high current regions are associated with enhanced dissipation [5,18–20]. A detailed and difficult analysis of the present simulation, beyond the scope of the present work, would be needed to attempt identification of specific microscopic dissipation mechanisms.

Here, to identify and statistically characterize regions that might contain elevated dissipation, we examine $D = \mathbf{J} \cdot \mathbf{E}$, the work done by electromagnetic fields on the particles. Conversion of magnetic energy into random kinetic energy must be contained in D, and since particles in collisionless plasmas interact only through the electromagnetic fields, dissipation must be contained in these measures. This identification is complicated by contributions from fluid motions, compressions, and reversible motions such as plasma oscillations. To reduce (but not eliminate) contributions due to fluid motions, we may evaluate D in a frame moving with either v_e or v_i. Here we also consider a related electron frame quantity $D_e = \mathbf{J} \cdot (\mathbf{E} + \mathbf{v}_e \times \mathbf{B}) - \rho_c (\mathbf{v}_e \cdot \mathbf{E})$, where $\rho_c = q(n_i - n_e)$ is the charge density [36]. A related interpretation of De is the work done by the nonideal part of the electric field in a generalized Ohm's law, corrected by removing the work associated with transport of the net charge.

In Fig. 4, we show the probability density functions of dissipation proxies: the electron frame dissipation measure D_e and $\mathbf{J} \cdot \mathbf{E}$. Both proxies have a broad and slightly asymmetric PDF. $\mathbf{J} \cdot \mathbf{E}$ has the broader distribution, as it includes additional contributions due to fluid scale stresses that exchange magnetic and flow energies. The slight preponderance of positive values in the distributions produce good agreement of global average values of dissipation $\langle D_e \rangle = 1.3 \times 10^{-7} c^3/d_e$, which compares well (within less than a factor of 2) with the computed decay of fluctuation energy (not shown).

The same figure shows the calculated average of dissipation D_e calculated based on the binned value of current density, and normalized by the global average dissipation rate $\langle D_e \rangle$. This normalized conditional average $\langle D_e | J \rangle$ is found to be a strongly increasing function of electric current density J. For example, in regions with current greater than 8 times its root mean square value, i.e., $J > 8 J_{\mathrm{rms}}$, the dissipation per unit volume is about 100 times the global average. Also shown are the same results from a 2.5D PIC simulation [19] that employed a different initial condition, but one that also leads to strong turbulence. It is interesting to notice that the 2D and 3D dissipation proxy curves agree well, at least up to $J = 6 J_{\mathrm{rms}}$, even though the present 3D simulation was initialized with isotropic fluctuations, while the 2.5D simulation created fluctuations self-consistently through instabilities. Evidently, the regions of enhanced coupling

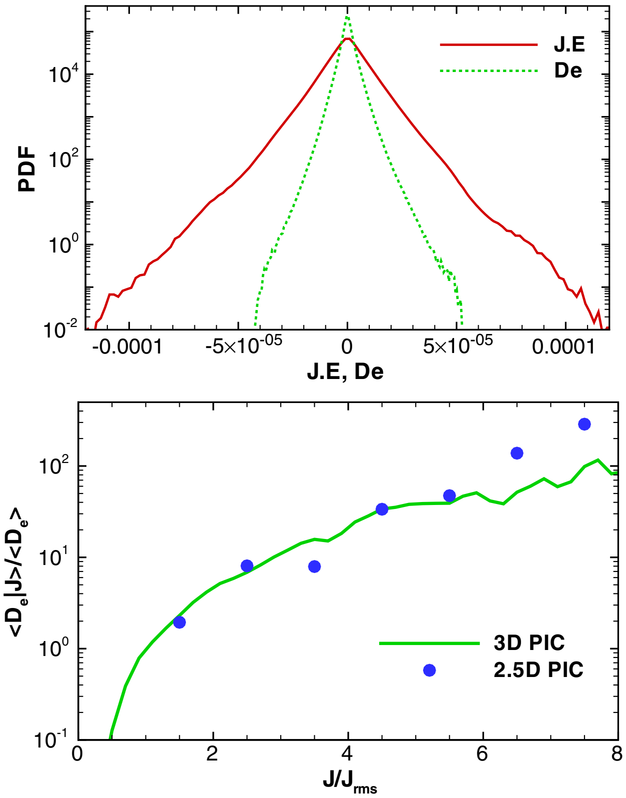

FIG. 4 (color online). (Top) PDFs of dissipation proxies: the electron frame dissipation measure D_e, $\mathbf{J}\cdot\mathbf{E}$. (Bottom) Conditional average of dissipation D_e calculated conditioning on the value of current density, normalized by the global average dissipation rate $\langle D_e\rangle$. Also shown are the same results from a 2.5D PIC simulation [19].

between the electromagnetic field and the particles can be dynamically concentrated in similar ways in 2.5D and 3D kinetic plasmas. This warrants further study using additional simulations.

A final issue that we consider relates to the heating of protons and electrons in regions of elevated current density. We recall that solar wind observations have suggested that proton heating (and to a lesser extent, electron heating) is elevated at strong magnetic gradients measured using the PVI method [22], and also in the vicinity of these gradients [37]. PIC simulations of 2.5D plasma turbulence find similar results [38]. We have examined what is essentially an analogous question—whether proton and electron temperatures are elevated in regions of strong currents. Figure 5 confirms this result for the present 3D PIC simulations, showing the averages of T_i and T_e conditioned on the strength of current density J, that is $\langle T|J\rangle$ where T is either the proton or electron temperature. Referring to the initial (equal) temperature also shown in the plot, we can see that both T_i and T_e have increased, while $T_e > T_i$ at the time of analysis for all values of J. However, we also note that the increase of conditionally averaged T_i with increasing J is greater than the increase of T_e with increasing J. Thus the

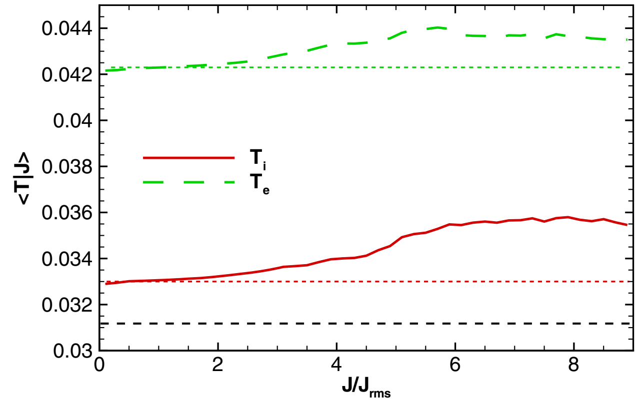

FIG. 5 (color online). Average of T_i and T_e conditioned on the strength of current density. The initial (equal) temperature of ions and electrons is plotted in dashed black line. The values of global T_i and T_e at the time of analysis are shown as reference dotted lines below the respective conditional averages. Both T_i and T_e are elevated in regions of stronger current density. Although electrons are hotter in general, the increase of T_i due to higher $|J|$ is greater than the increase of T_e due to higher $|J|$.

local elevation of proton temperature associated with stronger currents is greater than the analogous response of electrons, when heat conduction is ignored. This is consistent with a recent study based on 2.5D PIC simulations [27], which suggested that proton heating is enhanced, relative to electron heating, by stronger turbulence, which increases the gradients seen by protons at their characteristic gyroscales.

In conclusion, we have described for the first time, the nonlinear, turbulent behavior of a large 3D kinetic plasma using high resolution kinetic simulations [26]. The cascade is characterized by generation of highly structured and filamentary current sheets, extending through the range of scale between proton and electron inertial scales. Direct computation of the work done by the electromagnetic field on the particles reveals that dissipation is nonuniform, and is strongly associated with magnetic structures. We conclude that for 3D plasma turbulence, heating and dissipation are highly intermittent, similar to some reports based on reduced models [5,17–19]. In fact, it is somewhat remarkable that the concentration of the dissipation function D_e in the regions of high current density is so similar in the 3D and 2.5D cases shown in Fig. 4. While we make no claims of universality of this result, it does demonstrate the feasibility of attaining physically important conclusions based on lower dimensionality results, a possibility that is currently viewed as controversial [5,39]. Our conclusion is also supported by hybrid Vlasov-Maxwell (HVM) simulations [40].

Many of the properties obtained in this simulation also appear to be consistent with observations of solar wind turbulence at kinetic scales [3,8,41]. In particular, these results suggest that nonuniform dissipation in structures extending down to electron scales are likely sources of substantial heating in collisionless space plasmas, consistent with the analysis of magnetosheath observations [42], and analysis of solar wind inertial range statistics [22]. We remark that we have examined numerically the effects of varying mass ratio (m_i/m_e) and the speed of light in 2.5D simulations, and this has given us confidence about using the parameters chosen here for the 3D case. Further study of the intermittency properties at kinetic scales will be reported in a subsequent paper, while additional analyses of solar wind data would appear to be a desirable next step.

Research is supported by NSF AGS-1063439, AGS-1156094 (SHINE), Solar Probe Plus science team (ISIS/SWRI subcontract No. D99031L), NASA grants NNX14AI63G (Heliophysics Grandchallenge Theory). H. K. and V. R. are supported from the NASA Heliophysics Theory Program, NSF ATM-0802380 and EAGER 1105084. Simulations were performed on Blue Waters supercomputer, supported by NSF OCI-07-25070 and the state of Illinois.

[1] R. J. Leamon, W. H. Matthaeus, C. W. Smith, and H. K. Wong, Astrophys. J. **507**, L181 (1998).
[2] S. P. Gary and J. E. Borovsky, J. Geophys. Res. **109**, A06105 (2004).
[3] F. Sahraoui, M. L. Goldstein, P. Robert, and Y. V. Khotyaintsev, Phys. Rev. Lett. **102**, 231102 (2009).
[4] S. P. Gary, O. Chang, and J. Wang, Astrophys. J. **755**, 142 (2012).
[5] J. M. TenBarge, G. G. Howes, and W. Dorland, Astrophys. J. **774**, 139 (2013); J. M. TenBarge and G. G. Howes, Astrophys. J. Lett. **771**, L27 (2013).
[6] L. Matteini, P. Hellinger, S. Landi, P. M. Trávníček, and M. Velli, Space Sci. Rev. **172**, 373 (2012).
[7] B. A. Maruca, J. C. Kasper, and S. D. Bale, Phys. Rev. Lett. **107**, 201101 (2011).
[8] S. D. Bale, P. J. Kellogg, F. S. Mozer, T. S. Horbury, and H. Reme, Phys. Rev. Lett. **94**, 215002 (2005).
[9] S. R. Cranmer, Space Sci. Rev. **101**, 229 (2002).
[10] B. J. Vasquez, C. W. Smith, K. Hamilton, B. T. MacBride, and R. J. Leamon, J. Geophys. Res. **112**, A07101 (2007).
[11] P. D. Mininni, Phys. Rev. E **76**, 026316 (2007).
[12] P. D. Mininni, A. Alexakis, and A. Pouquet, Phys. Rev. E **77**, 036306 (2008).
[13] S. Saito, S. P. Gary, H. Li, and Y. Narita, Phys. Plasmas **15**, 102305 (2008).
[14] T. N. Parashar, M. A. Shay, P. A. Cassak, and W. H. Matthaeus, Phys. Plasmas **16**, 032310 (2009).
[15] D. Verscharen, E. Marsch, U. Motschmann, and J. Muller, Phys. Plasmas **19**, 022305 (2012).
[16] E. Camporeale and D. Burgess, Astrophys. J. **730**, 114 (2011).
[17] S. Servidio, F. Valentini, F. Califano, and P. Veltri, Phys. Rev. Lett. **108**, 045001 (2012).
[18] T. N. Parashar, S. Servidio, M. A. Shay, B. Breech, and W. H. Matthaeus, Phys. Plasmas **18**, 092302 (2011).
[19] M. Wan, W. H. Matthaeus, H. Karimabadi, V. Roytershteyn, M. Shay, P. Wu, W. Daughton, B. Loring, and S. C. Chapman, Phys. Rev. Lett. **109**, 195001 (2012).
[20] H. Karimabadi *et al.*, Phys. Plasmas **20**, 012303 (2013).
[21] W. Daughton, V. Roytershteyn, H. Karimabadi, L. Yin, B. J. Albright, B. Bergen, and K. J. Bowers, Nat. Phys. **7**, 539 (2011).
[22] K. T. Osman, W. H. Matthaeus, A. Greco, and S. Servidio, Astrophys. J. Lett., **727**, L11 (2011); K. T. Osman, W. H. Matthaeus, B. Hnat, and S. C. Chapman, Phys. Rev. Lett. **108**, 261103 (2012).
[23] A. Retinò, D. Sundkvist, A. Vaivads, F. Mozer, M. André, and C. J. Owen, Nat. Phys. **3**, 236 (2007).
[24] S. Perri, M. L. Goldstein, J. C. Dorelli, and F. Sahraoui, Phys. Rev. Lett. **109**, 191101 (2012).
[25] K. J. Bowers, B. J. Albright, L. Yin, B. Bergen, and T. J. T. Kwan, Phys. Plasmas **15**, 055703 (2008).
[26] V. Roytershteyn, H. Karimabadi, V. M. Uritsky, A. Roberts, W. H. Matthaeus, G. De Vita, L. Sorriso-Valvo, W. Daughton, and M. Wan (to be published).
[27] P. Wu, M. Wan, W. H. Matthaeus, M. A. Shay, and M. Swisdak, Phys. Rev. Lett. **111**, 121105 (2013).
[28] J. V. Shebalin, W. H. Matthaeus, and D. C. Montgomery, J. Plasma Phys. **29**, 525 (1983).
[29] S. Oughton, E. R. Priest, and W. H. Matthaeus, J. Fluid Mech. **280**, 95 (1994).
[30] J. W. Bieber, W. Wanner, and W. H. Matthaeus, J. Geophys. Res. **101**, 2511 (1996).
[31] F. Sahraoui, M. L. Goldstein, G. Belmont, P. Canu, and L. Rezeau, Phys. Rev. Lett. **105**, 131101 (2010).
[32] S. Oughton, W. H. Matthaeus, M. Wan, and K. T. Osman, Proc. R. Soc. A **373**, 20140152 (2015).
[33] E. Leonardis, S. C. Chapman, W. Daughton, V. Roytershteyn, and H. Karimabadi, Phys. Rev. Lett. **110**, 205002 (2013).
[34] D. Biskamp, Plasma Phys. Controlled Fusion **26**, 311 (1984).
[35] T. Yokoyama and K. Shibata, Astrophys. J. **436**, L197 (1994).
[36] S. Zenitani, M. Hesse, A. Klimas, and M. Kuznetsova, Phys. Rev. Lett. **106**, 195003 (2011).
[37] K. T. Osman, W. H. Matthaeus, M. Wan, and A. F. Rappazzo, Phys. Rev. Lett. **108**, 261102 (2012).
[38] P. Wu, S. Perri, K. Osman, M. Wan, W. H. Matthaeus, M. A. Shay, M. L. Goldstein, H. Karimabadi, and S. Chapman, Astrophys. J. Lett. **763**, L30 (2013).
[39] G. G. Howes, J. Plasma Phys. **81**, 325810203 (2015).
[40] S. Servidio, F. Valentini, D. Perrone, A. Greco, F. Califano, W. H. Matthaeus, and P. Veltri, J. Plasma Phys. **81**, 325810107 (2015).
[41] O. Alexandrova, V. Carbone, P. Veltri, and L. Sorriso-Valvo, Astrophys. J. **674**, 1153 (2008).
[42] D. Sundkvist, A. Retino, A. Vaivads, and S. D. Bale, Phys. Rev. Lett. **99**, 025004 (2007).